



Hydrological uncertainties in the modelling of cave drip-water $\delta^{18}\text{O}$ and the implications for stalagmite palaeoclimate reconstructions

Chris Bradley^{a,*}, Andy Baker^{b,c}, Catherine N. Jex^a, Melanie J. Leng^{d,e}

^a School of Geography, Earth and Environmental Sciences, University of Birmingham, Birmingham B15 2TT, UK

^b Connected Waters Initiative, UNSW, 110 King St, Manly Vale, NSW 2093, Australia

^c The National Centre for Groundwater Research and Training, GPO Box 2100, Adelaide, SA 5001, Australia

^d NERC Isotope Geosciences Laboratory, British Geological Survey, Keyworth, Nottingham NG12 5GG, UK

^e School of Geography, University of Nottingham, Nottingham NG7 2RD, UK

ARTICLE INFO

Article history:

Received 22 January 2010

Received in revised form

11 May 2010

Accepted 13 May 2010

ABSTRACT

In this paper we review our current understanding of karst drip-water hydrology, emphasising the extent of non-linear and non-stationary process dynamics that render stalagmite palaeoclimate reconstructions using a statistical pseudo-proxy approach difficult to implement. We outline an approach to attribute the uncertainty that arises specifically as a consequence of variable water routing through the overlying soil, epikarst and karst aquifer. This is based upon the development of a monthly lumped parameter karst hydrological model which we use to demonstrate the range of modelled drip-water discharges possible from a single climate input. Refinement of the model, to include precipitation $\delta^{18}\text{O}$, enables us to determine the theoretical range in drip-water and stalagmite $\delta^{18}\text{O}$ for three sites with contrasting climates: northern temperate (NW Scotland), monsoonal (Ethiopia), and Mediterranean (Gibraltar). For actual climate (monthly mean temperature; monthly total precipitation; monthly mean precipitation $\delta^{18}\text{O}$), we compare model simulations of karst groundwater storage and drip-water $\delta^{18}\text{O}$ to demonstrate our ability to model different climate regimes realistically. We also investigate the $\delta^{18}\text{O}$ variability associated with specific karst water reservoirs that differ in their capacity and drainage mechanisms. $\delta^{18}\text{O}$ variability is then compared to stalagmite $\delta^{18}\text{O}$ record from the three regions for the last ~45 years. We conclude by reviewing the implications of our hydrological model for stalagmite $\delta^{18}\text{O}$ Quaternary palaeoclimate reconstructions over different timescales and sampling resolutions.

© 2010 Elsevier Ltd. All rights reserved.

1. Introduction

Speleothem deposits have provided abundant palaeoclimate data, yielding well-dated, long-term, high resolution data which can validate the output of general circulation models, particularly for events characterised by a high signal to noise ratio such as glacial/inter-glacial transitions (McDermott, 2004). In recent years, speleothem data series have contributed to the development of multi-proxy records that have greatly increased our understanding of changes in the global climate system. These have drawn upon advances in a number of related areas, including sample processing (micro-drilling; Spötl and Matthey, 2006); analytical developments; and understanding of the wider 'climatic and environmental' controls on oxygen isotope ($\delta^{18}\text{O}$) values (Lachniet, 2009). Together

these have substantially enhanced our ability to use information from stalagmites to reconstruct Quaternary climates, however, a number of research problems and questions remain outstanding. These include the degree of uncertainty in speleothem $\delta^{18}\text{O}$ records which are especially apparent over periods of relatively stable climate, but which have largely yet to be fully quantified, emphasising the importance of improving our understanding of data variability or quantification of the 'noise' that is commonly found. For example, Cheng et al. (2009) report ~4‰ variations in $\delta^{18}\text{O}$ over glacial-interglacial cycles but with an un-interpreted high frequency (approximately decadal) variability of <1‰, with an analytical error of ~0.05‰. Uncertainty in speleothem records arises in a number of ways (McDermott, 2004; Fairchild et al., 2006a; Lachniet, 2009) and is at least partly a reflection of the natural environmental variability that typifies karst terrain at different scales. However, it also reflects inadequate and incomplete understanding, and the dynamic behaviour of karst systems, particularly with respect to process inter-relationships. These contribute to uncertainty at several levels given the relationship

* Corresponding author. Tel.: +44 1214148097; fax: +44 1214145528.

E-mail addresses: c.bradley@bham.ac.uk (C. Bradley), a.baker@unsw.edu.au (A. Baker), c.jex@bham.ac.uk (C.N. Jex), mjl@bgs.ac.uk (M.J. Leng).

(and inter-dependence) between drip-water hydrology (i.e. water flow pathways and water chemistry), surface and sub-surface climatology (surface recharge, evapotranspiration etc.), and speleothem $\delta^{18}\text{O}$.

Recent advances in speleothem research and in their wider application (improved systems understanding; high precision ICP-MS dating; long continuous $\delta^{18}\text{O}$ records; Fairchild et al., 2006a; Hoffmann, 2008; Wang et al., 2008; Cheng et al., 2009) reflect our increasing ability to constrain more closely speleothem output time-series given the developments noted above, in addition to concurrent advances in our understanding of the geomorphology, hydrology and hydrogeology of karst systems (White, 2002; Ford and Williams, 2007; Worthington and Gunn, 2009). Together these advances have helped unravel some of the complexities that characterise the multi-determinate karst-climate system but specific error attribution remains problematic. Accordingly, in this article we describe a parsimonious approach to investigate hydrological uncertainties in speleothem $\delta^{18}\text{O}$ that are associated specifically with the dynamics of drip-water flow in cave systems. Empirical results suggest that speleothem drip rates are frequently characterised by non-linear behaviour as a result of temporally variable recharge to the karst coupled with non-linear water movement at various scales to the stalagmite (Baker and Brunson, 2003). Here we examine the physical processes that determine water routing through the overlying soil, epikarst and karst aquifer using a lumped hydrological model to describe potential inter-relationships between waters routed at different rates between individual sub-surface water stores that differ in their size and drainage characteristics. Given difficulties of model verification, and the likely variability in hydraulic parameters between karst regions (Bakalowicz, 2005), we aim to demonstrate the potential of a generic modelling approach that avoids intractable problems such as site-specific model calibration, but which enables us to perform a sensitivity analysis to quantify hydrological uncertainty across a range of karst systems. Our ultimate aim is for the modelling approach developed here to be used to drive forward models of stalagmite $\delta^{18}\text{O}$ (Sturm et al., 2009; Baker and Bradley, 2010) and ultimately to generate stalagmite $\delta^{18}\text{O}$ pseudoproxies (Moberg et al., 2008).

2. Karst hydrology

Karst is a heterogeneous, and in some cases, highly fractured, carbonate rock in which the permeability of the substrate has developed over time to the extent that the majority of water movement occurs below the surface. Point and diffuse seepage of autogenic and allogenic waters (*sensu* Gunn, 1983) associated with surface precipitation and point surface-water inflows, progressively enhance structural voids and conduits through carbonate dissolution. Over extended periods of time (in excess of 50 ky), this leads to the formation of karst, which is associated with dense, massive, and frequently coarsely-fractured, limestone and dolomite, within which three levels of porosity can be distinguished (Ford and Williams, 2007). Primary porosity, in the (bed)rock, is generally limited and related to inter-granular void space, while secondary porosity is associated with joints and fractures, and tertiary porosity with solution-enhanced conduits. Depending upon the connectivity between individual structures in the karst, a continuum of sub-surface water flow pathways may be envisaged that range between rapid, preferential, flow through interconnected conduits, to slower matrix flow (Shuster and White, 1971; Newson, 1973). Actual water flow pathways will vary according to the delivery of water to the karst drainage system which may be difficult to define accurately and will also reflect the connectivity between structural voids within the karst, the degree

to which the permeability has developed over time, and the configuration of karst water stores, whether within the matrix, or structural voids within the karst.

Hypothetical karst water flow pathways are illustrated schematically in Fig. 1, showing possible mechanisms by which water might be delivered to individual speleothems. The simplest pathway is associated with Stalagmite A, which is fed solely by diffuse matrix flow. In this case, water movement will be a function of the primary porosity of the karst, with flow rates proportional to the matrix permeability. In contrast, Stalagmite B is fed by both matrix and preferential (fissure) components of flow, and drip rates are likely to vary over time, depending upon the mode of water delivery to the preferential flow system. Drip-waters associated with Stalagmites C and D also include matrix and preferential flow, but here a proportion of flow is routed through a water reservoir, or store, in the epikarst or karst. These water stores may function in different ways: varying in their capacity and in the mode with which they fill and drain. Thus, preferential flow to stalagmite C is routed through one water store (1), which drains by 'underflow', and the stalagmite also receives some matrix flow. In contrast, Stalagmite D receives waters from a 'overflow' storage reservoir (3), which is itself filled by seepage from a second water store (2). Water fluxes to Stalagmite D are likely to be discontinuous over time, occurring at times when the water storage volume exceeds a certain threshold, and with flux rates that vary according to the characteristics of the outlet point(s). In summary, percolating waters may follow a variety of flow pathways through karst depending upon the configuration of the drainage system, although the surface-water balance, including rates of evapotranspiration, precipitation, and water storage within the epikarst determine the delivery of water to individual karst flow systems (Williams, 2008).

Multiple combinations of the flow pathways represented in Fig. 1 can be envisaged. Potentially there may be many individual water stores within the karst, epikarst and soil systems, with percolating waters routed between stores by pathways that range from rapid, turbulent, preferential flows through large interconnected conduits, to slow, diffuse seepage through smaller fissures or voids in the karst. It is very likely, therefore, that individual speleothems within the same cave system may differ markedly in how their drip-waters have been routed, which accounts for the variety of stalagmite shapes that are commonly observed (Franke, 1965; Dreybrodt and Lamprecht, 1981; Gams, 1981; Dreybrodt and Franke, 1987). Thus, candlestick or minimum 'diameter', stalagmites (A in Fig. 1) are fed by drips with a relatively constant flow regime that limits flow and carbonate precipitation along the flanks of the speleothem. In contrast, larger stalagmites, such as 'bosses' or those with a complex morphology (B, C, D in Fig. 1), indicate a temporally variable drip-water flow regime with high flow down the flank of the stalagmite and carbonate precipitation along the margins. However, the majority of stalagmites show no dramatic change in their morphology over time, indicating that these hydrological processes (i.e. the mechanisms and flow pathways associated with individual speleothems) can essentially be regarded as time-invariant over millennial timescales.

There is, however, a range of empirical evidence that highlights the dynamics of karst water movement from detailed field observation. Early studies described seasonal variations in drip-water hydro-chemistry at de Poole Cavern, Derbyshire, UK, over a 12-month period (Pitty, 1966, 1968), while monitoring of drip-water variability over an annual cycle (including drip-water discharge and the coefficient of variation (CV)) demonstrated that most stalagmite drip-waters are characterised by a discharge of $<10^{-5} \text{ l s}^{-1}$ and a CV of between 10 and 200% (Smart and Friederich, 1987; Baker et al., 1997; Baker and Barnes, 1998). Higher CVs were associated

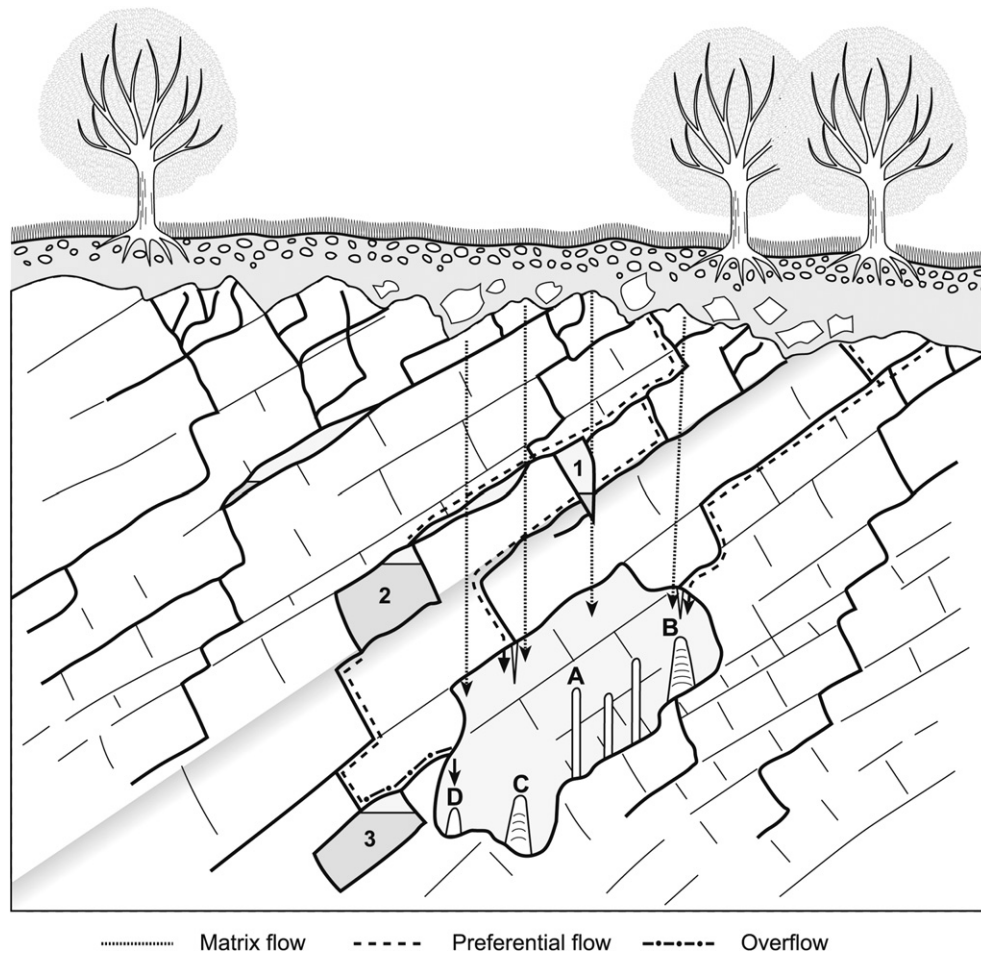


Fig. 1. Schematic illustration of possible karst water flow pathways to four hypothetical speleothems (A, B, C, D) and their relationship to three water reservoirs (1, 2, 3).

with drip-waters that displayed a significant seasonal variation in flow regime, with an apparent increase in the proportion of seepage waters routed via preferential flow as CV increases. Although relatively little drip-water data are currently available, these results suggest that some stalagmites may be fed by drip-waters that are entirely a product of diffuse seepage through the karst, whilst in other cases drip-waters may include a (varying) combination of diffuse and preferential flow (Genty and Deflandre, 1998; Baker and Brunson, 2003). For example, Genty and Deflandre (1998) monitored drip-waters below a stalactite in the Père Noël cave, S. Belgium, for >5 years and identified periods of water flushing from the soil or epikarst, indicating piston, or displacement, flow with sequential water movement through linked water stores. Additional high frequency, low amplitude, variations in drip-water discharge were inversely correlated with air pressure, suggesting two-phase flow. These dynamic variations in karst water routing, and their variability between individual stalagmites and over time, have important implications for speleothem research, influencing, for example, solute concentrations, including karst Mg/Ca ratios, and affecting the dynamics of carbonate precipitation.

3. Environmental constraints on drip-water isotopic composition

To a certain extent, it should be possible to infer changes in water residence time, in flux rates and the relative proportions of

matrix and preferential flow from stable isotopes. However, whilst the dynamics of karst water movement also have significant implications for stalagmite $\delta^{18}\text{O}$, these have proved difficult to distinguish from the wider environmental controls on $\delta^{18}\text{O}$ that have been reviewed by Lachniet (2009). The isotopic composition of drip-waters also reflects other variables including: atmospheric inputs, evaporation and soil profiles as well as the local hydro-geology, and sampling techniques. In general, the spatial and temporal patterns of $\delta^{18}\text{O}$ in precipitation, and their relationship to climate processes, are very well understood (for example see Gat, 1996; Bowen and Wilkinson, 2002; Lachniet, 2009) such that water isotopes have been integrated into general circulation models (e.g. LeGrande and Schmidt, 2009; Sturm et al., 2009; Noone and Sturm, 2010). The first-order controls on soil-water isotopic composition are atmospheric inputs (precipitation), evaporation, and the soil physical properties that control soil-water movement and storage (Shurbaji and Phillips, 1995). Thus isotope analyses of soil-waters sampled at different depths through the soil-groundwater system will generate a typical depth profile that is characterised by an evaporative effect near the surface with enrichment in deuterium and ^{18}O , but with rates that diminish and are increasingly smoothed with depth (Zimmerman et al., 1967; Tang and Feng, 2001). These trends with depth are a function of climate, the rate of drainage, the soil-water storage capacity, and may potentially be affected by lateral water movement and soil salinisation. Thus soil structure, particularly the saturated and unsaturated hydraulic conductivity, and soil porosity, is an

important factor controlling rates of water movement, whilst the wider geomorphological and hydrogeological setting will also influence patterns of sub-surface water flow and drainage.

Soil-water isotopic compositions are also likely to vary according to the residence time of the waters sampled, the initial $\delta^{18}\text{O}$ composition of the component rain events, and fractionation from evaporation (Robertson and Gazis, 2006). The bulk soil-water $\delta^{18}\text{O}$ composition will be influenced by antecedent moisture contents, and the proportion of extracted soil-waters (if any) that may have been previously adsorbed onto soil particles rather than held within open soil pores. Soil-water isotopic compositions may also vary depending upon the technique used to extract water samples in the field, particularly whether samples were collected by gravity drainage, or using suction lysimeters. For the latter, the water residence time is likely to be longer, and is more likely to include a proportion of soil-waters that were formerly absorbed onto soil minerals.

The isotopic composition of precipitation varies significantly, seasonally and within individual rain events. Within-event rainfall $\delta^{18}\text{O}$ variations in excess of 10‰ have been observed (Celle-jeanton et al., 2001) which may lead to different water isotopic inputs to individual components of the karst water flow systems, such as fracture, macro-pore, and matrix in the soil, epikarst and karst. Soil isotopic composition will also depend upon drainage rates, and although infiltration capacities are probably seldom exceeded in karst areas, the partitioning of rainfall between diffuse and preferential drainage pathways will reflect the characteristics of the rainfall event, and antecedent moisture levels. Moreover, at both seasonal and inter-annual timescales, changes in atmospheric $\delta^{18}\text{O}$ input and evapotranspiration will generate variations in surface soil-water isotope enrichment which it is important to quantify. In some environments there may be significant source-water evaporation to the atmosphere which can be traced using water isotopes. The amount of surface isotope enrichment has been shown to vary with evaporation although transpiration does not fractionate soil-water, except for hydrogen isotopes during uptake by some halophytes. At present these relationships are poorly constrained with very few monitoring studies, although Hsieh et al. (1998) found soil-water enrichment at a depth of 20 cm of $\sim 6.5\%$ for potential evapotranspiration (PET) of 4.5 mm/day and $\sim 2.0\%$ for 1 mm/day PET in samples collected from four soils along a bioclimatic transect in Hawaii (their Fig. 8).

In summary, speleothem $\delta^{18}\text{O}$ can be regarded as an integrated product of some or all of the processes reviewed in this section. The extent to which high frequency, low amplitude variations in speleothem $\delta^{18}\text{O}$ are a simple product of a climate signal (e.g. a direct response to precipitation) or a product of the uncertainty associated with the soil or karst hydrology remains to be determined. A particular research gap is the incorporation of hydrological variability into our understanding of speleothem $\delta^{18}\text{O}$. Given the number and complexity of processes involved over a range of timescales, a modelling approach is reviewed in detail here.

4. Modelling karst hydrology and drip-water flow

While drip-water $\delta^{18}\text{O}$ composition reflects the environmental constraints summarised above, the attribution of differences in $\delta^{18}\text{O}$, both over time and between speleothems, that arises specifically as a result of karst water routing is problematic given the difficulty in determining the configuration of any karst drainage system. However, models of varying complexity can clarify some of the process inter-relationships that typify the karst environment, and their implications for $\delta^{18}\text{O}$ composition, as they enable selected parameters to be constrained within a simplified representation of

the karst system. In this sense, a model enables the relationships between key processes to be formalised with a view to addressing a particular area of interest. Thus models have been used for predictive purposes, to interpret or explain specific attributes of system behaviour, whilst generic models may be used to address hypothetical questions and inter-relationships. Ultimately, model selection will depend upon the purpose of the study, and karst systems have been modelled at many levels to consider individual facets of the karst environment.

Early models of karst systems sought to describe key characteristics of water movement. Thus at a generic, or conceptual, level, Gunn (1974) described the routing of drip-water flows by conduit and diffuse flow between individual soil and groundwater stores at Waterfall Swallet, Derbyshire, UK. This developed earlier research by White (1969) who had highlighted the variety of karst water fluxes ranging from laminar, diffuse, flow, through the matrix, to turbulent conduit flow. Individual models of water movement through karst have apportioned water flow between conduit (preferential) and diffuse (matrix) flow components in different ways. To a certain extent their success depends upon their ability to provide inputs of water to the karst flow system at the appropriate time (and volume). However, the results and methods are also scale-dependent, and reflect differences in the original purpose of the modelling exercise, although speleothem drip data can help verify estimates of groundwater recharge (e.g. Sanz and López, 2000). Typically, investigations of karst water resources have been at a wide spatial scale and have focussed on spring and/or borehole level data for model verification as reviewed by Taylor and Greene (2008). Thus karst spring response to individual recharge (precipitation) events have been quantified using impulse response functions, that circumvent practical difficulties in parameterising a full karst model by analysing discharge series to relate an input series (precipitation) to the output (spring flow) that provides an integrated description of karst hydrology (e.g. Pinault et al., 2001). These methods appear to be particularly suited to situations where the karst is relatively mature, where they represent a form of 'black box' model, where discharge, recharge and geochemical data can be used initially to quantify the inter-relationships, and subsequently for model verification. However, these types of model, whilst clarifying bulk flow properties, have only a limited potential to characterise local variability in water movement and storage; which are frequently important to quantify for speleothem research.

Irrespective of the model objectives, karst hydrology models require a gross-simplification of the karst system, particularly given the difficulty in characterising *inter alia* karst permeability, porosity, specific storage, pore connectivity, and ultimately, in validating model results. For many applications, spatial scale is critical as illustrated by the 'representative elementary volume' (REV) concept, defined by Bear (1972) as the volume of a medium that is sufficiently large to eliminate erratic fluctuations in macroscopic properties. Thus, although karst aquifers are markedly heterogeneous, standard porous media models may provide an adequate description of the macro-scale groundwater potentials at greater spatial scales. Teutsch (1993) has suggested that standard porous media models can be used to model karst hydrology, with both primary and secondary porosity (and permeability) represented as an equivalent continuous porous medium for a particular REV. This suggests that in some situations it may be possible to use proprietary finite-difference/finite element groundwater models to describe water flow through karst, although as for the black box models discussed above, groundwater models at this scale are unlikely to clarify individual water flow paths and their variability. At a conceptual level, however, such models can be used to investigate patterns of water flow and variations in piezometric levels.

For example, [Worthington and Ford \(2009\)](#) used a finite-difference groundwater model to examine the configuration of a karst conduit network. However, where karstification is more advanced, and greater proportions of water are routed through the conduit network, dual porosity models have proved successful, for situations as described by [Atkinson \(1977\)](#) who found 60–80% of flow was preferential. Alternatively, some models have concentrated entirely on flow through the karst fracture system, assuming that water flow only occurs through the fracture network (e.g. [Adams and Parkin, 2002](#)).

Given the difficulty in parameterising individual models, and the desirability of focussing on certain key aspects of karst system behaviour, a compromise approach is frequently required, as illustrated by applications using lumped parameter models. In theory, such models are easier to develop as difficulties in describing spatial variations in key processes are avoided, and hence significantly fewer model parameters are required. Lumped models are commonly used in hydrology, and karst systems have been modelled successfully in this way. Thus [Barrett and Charbeneau \(1997\)](#) modelled flow through the 400 km² Edwards Aquifer, Texas, using five groundwater cells, each of which represented an individual surface-water catchment, with inter-cell flows estimated using Darcy's Law. Other applications of lumped parameter, or reservoir, models of karst hydrology include [Thiéry \(1988\)](#), [Long \(2009\)](#) and [Fleury et al. \(2007\)](#). In the latter study, [Fleury et al.](#) modelled the Fontaine de Vaucluse karst system, NW Provence, France, over a 10-year period by describing the filling and drainage of two distinct reservoirs that sustain slow and rapid components of karst stream flow.

Recent developments in modelling karst hydrogeology, and concurrent advances in instrumentation for automatic logging of drip-water discharge, have yet to lead to more sophisticated models of stalagmite drip-water hydrology. There is considerable potential for work in this area, particularly given the increasing scope to verify model predictions in different ways. For example, [Yamada et al. \(2008\)](#) estimated the age of water extracted from individual straw stalactites in two caves in Sukabumi, East Java using ³H/³He as 12.9 ± 3.8 and 13.5 ± 6.3 yrs. They compared these results to ages estimated by modelling water infiltration rates using Darcy's Law (permeabilities: 0.71 × 10⁻⁷ and 1.31 × 10⁻⁷ m/s; porosity of 20%) from which they obtained a modelled age for the diffuse flow component of 8–13 yrs (both caves were ~30–50 m deep and 3.75 m/yr linear vertical velocity assumed). In another study, [Fairchild et al. \(2006b\)](#) developed a numerical model based upon the seepage and fracture flow components described *inter alia* by [Smart and Friederich \(1987\)](#) and an integrated soil and groundwater conceptual model of [Tooth and Fairchild \(2003\)](#). Their two layer model consisted of an upper layer (representing the soil and epikarst) and a lower mixing layer, with water routed between the two layers via a combination of linear reservoirs. Driven by surface hydrology, the model sought to predict both stalagmite drip hydrology and major cation chemistry; however, it failed to predict successfully both hydrology and cation concentrations in situations of non-linear flow. This suggests that a relatively simple two layer linear reservoir approach (i.e. a lumped parameter model) failed to represent the system adequately in this instance. A similar model is presented in [Baker et al. \(in press\)](#), where the δ¹⁸O record of a modern growth phase of an Ethiopian stalagmite was modelled using a single reservoir. In this instance, stalagmite δ¹⁸O could be successfully modelled by an overflow routing from a single reservoir. However, such models are commonly site-specific and are effectively uniquely calibrated to describe water movement to a single speleothem in one cave system. More sophisticated approaches are necessary to describe the variety of water flow pathways, and storage reservoirs and accordingly in the next section we present a more complex karst hydrological model.

4.1. KarstHydroMod – a stalagmite δ¹⁸O forward model

A stalagmite drip-water model has been developed to simulate the implications of hypothetical configurations of the karst drainage system for stalagmite δ¹⁸O. Water flows are envisaged to occur by a combination of matrix, and preferential (fissure and conduit) flow between discrete water stores as illustrated schematically in [Fig. 2](#) which summarises the relationship between individual water reservoirs in the epikarst and karst and matrix and preferential (fissure and conduit) flows. Each water reservoir is associated with a particular δ¹⁸O composition which is determined by a simple mixing model as a function of the δ¹⁸O composition of source precipitation and the δ¹⁸O composition of the reservoir at the previous time-step. Initial δ¹⁸O is thus derived from precipitation and transformed by evaporative fractionation in the soil ($^{18}\text{O} = ^{18}\text{O} + (\text{evap} \times 0.03)$) mixing between waters of varying residence time within the reservoirs, and finally temperature dependent fractionation when incorporated into a stalagmite. Fractionation is assumed to occur only in the near-surface reservoir (within the epikarst) due to evaporation. Water routing through the system is a function of the hydrologically-effective precipitation (precipitation minus evapotranspiration) in each time-step, and the volume of water in each storage reservoir. Near-surface water movement is also restricted at times when the temperature is <0 °C to represent temporary surface-water storage as snow and ice. Essentially the model enables surface-water inflows to be partitioned between diffuse and preferential flows, depending upon the distribution of effective precipitation over time, and the capacity and volumes of water stored in each reservoir at a particular time.

The principal hydrological variables in the model are summarised in [Table 1](#). The main water fluxes and reservoirs are inter-dependent, and variable routing of percolating waters is envisaged between two surface/sub-surface water stores (*Surface Store*; *Epikarst*) and three karst water reservoirs (*Store 1*, *Overflow Store*, *Underflow Store*), each of which potentially represents a source of speleothem drip-waters. Near-surface water storage (*Surface Store*) may reflect impeded drainage as a result of sub-zero temperatures and the seasonal accumulation of surface snow and ice, or high precipitation in excess of the infiltration capacity. Percolating waters may also be stored temporarily within the *Epikarst*. Of the water stores, the *Epikarst* has a defined capacity, as does *Store 1* where the capacity is limited by the initiation of overflow drainage above a certain threshold volume. The remaining water stores have no maximum value, and are regulated by the balance between water inflows and outflows. The latter are defined by a proportional drainage function that allows the outflow to vary according to the volume of water stored at any time, with drainage volumes falling progressively when storage volumes diminish at times of reduced groundwater recharge. Theoretically, individual speleothems might receive drip-waters that have followed distinctly different pathways through the karst (i.e. 50% from *Store 1* and 50% from *Underflow*; or: 25% diffuse seepage from *Epikarst*, and 75% from *Overflow*), and within the same case system, drip-waters can be expected to vary markedly. Actual water flow pathways are largely determined by the quantity of waters stored in key reservoirs at a particular time, and the magnitude of the hydrologically-effective precipitation.

The model, as described above and summarised in [Table 1](#), was developed by a trial-and-error process in ModelMaker 4.0 ([Walker and Crout, 1997](#)) and requires four input files: precipitation, evapotranspiration, temperature and the δ¹⁸O composition of precipitation. The initial model configuration was designed using monthly hydrological data from Gibraltar and concentrated upon ensuring that the model continues to provide drip-water supply under a variety of conditions (i.e. periodic drought; changes in the magnitude and frequency of precipitation), and with water stores

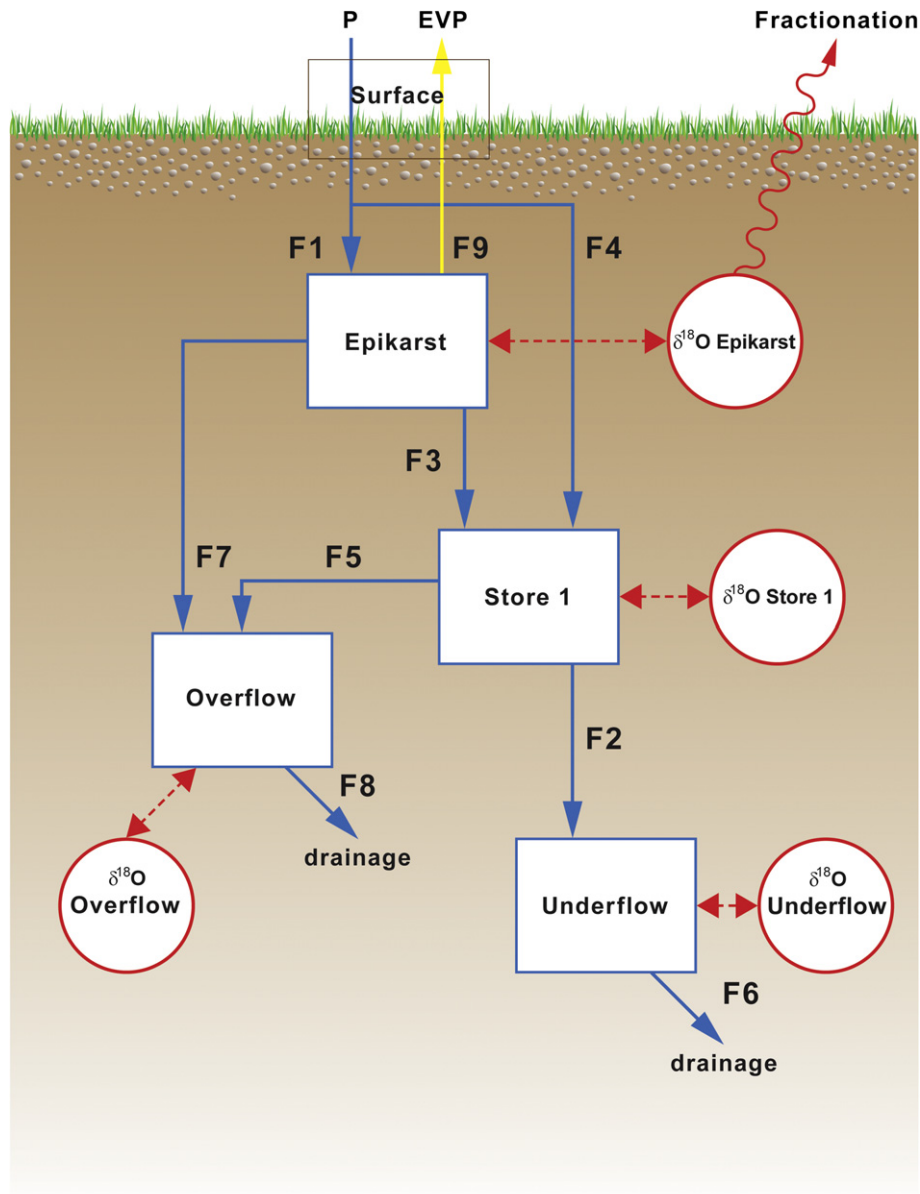


Fig. 2. Conceptual model of karst hydrology and relationship between water flow pathways to $\delta^{18}\text{O}$ variations in individual karst water reservoirs.

that never drain completely. Inevitably, many combinations of water flow pathways and stores may exist in practice, and hence it might only be possible to ‘calibrate’ a particular model configuration for one speleothem in one cave system. However, it is possible to examine model performance at a generic level under different climatic regimes that are representative of particular karst provinces to confirm that the model continues to provide drip-waters under a variety of conditions. A theoretical karst hydrology model also enables the potential variability (and hence uncertainty) in $\delta^{18}\text{O}$ composition between individual reservoirs to be quantified, whilst ultimately the model results can be verified by comparing modelled speleothem $\delta^{18}\text{O}$ with data from actual stalagmites. Thus in this paper we develop the model analysis by using the same model configuration to predict $\delta^{18}\text{O}$ series for speleothems in three contrasting climatic regions for which stalagmite $\delta^{18}\text{O}$ records have been published. For a temperate maritime climate, we consider NW Scotland, where 1000 year reconstructions of precipitation and the North Atlantic Oscillation have been derived from stalagmite

annual lamina width (Proctor et al., 2000; Trouet et al., 2009) and precipitation, drip-water and modern stalagmite $\delta^{18}\text{O}$ published (Fuller et al., 2008). For a Mediterranean climate, we consider Gibraltar, from where a high resolution stalagmite $\delta^{18}\text{O}$ record was recently published (Mattey et al., 2008) and which has been the focus of a previous hydrological modelling effort (Baker and Bradley, 2010). Finally, for a monsoon climate we consider Ethiopia, the focus of recent attempts to calibrate stalagmite $\delta^{18}\text{O}$ (Baker et al., 2007, in press) and only recently recognised as experiencing a summer East African monsoon (Segele et al., 2009). This is described in the following section which looks at the implications of differences in the dynamics of water movement and storage for speleothem $\delta^{18}\text{O}$ composition.

4.2. Modelled karst water dynamics and $\delta^{18}\text{O}$ composition

For each site input files were prepared to summarise the monthly water budget over the 25-year period from 1980 to 2004.

Table 1

Summary description of how the principal water reservoirs and water fluxes are configured within the karst hydrology model.

| Water reservoirs | |
|------------------|---|
| Surface store | Sole inflow is 'hydrologically-effective' precipitation (Precipitation minus Evapotranspiration); Outflows are <i>F1</i> and <i>F4</i> . This store retains water whenever temperatures are $<0^{\circ}\text{C}$. |
| Epikarst store | Receives flow from the <i>Surface</i> (<i>F1</i>), outflows are evapotranspiration (when precipitation minus evapotranspiration <0); diffuse seepage (<i>F3</i>) to <i>Store 1</i> ; and preferential flow to <i>OverFlow Store</i> . The <i>Epikarst</i> has a defined capacity Epi_{max} : 75 mm |
| Store 1 | Principal karst water reservoir. Receives diffuse flow from the <i>Epikarst</i> (<i>F3</i>) and preferential flow directly from the <i>Surface</i> (<i>F4</i>). Outflows are drainage (<i>F4</i>) and an overflow (<i>F5</i>) whenever the volume of water stored (in <i>Store 1</i>) exceeds 120 mm. Initial storage volume is 50 mm. |
| OverFlow store | Receives preferential flow from the <i>Epikarst</i> (<i>F7</i>) and overflow from <i>Store 1</i> (<i>F5</i>). Only outflow is drainage (<i>F8</i>). Initial storage volume is 50 mm. |
| UnderFlow store | Receives inflow from <i>Store 1</i> (<i>F2</i>) and only outflow is drainage (<i>F6</i>). Initial storage volume is 100 mm. |
| Water fluxes | |
| <i>F1</i> | Water movement only occurs when the temperature is $>0^{\circ}\text{C}$. All water from the surface is allowed to flow to the <i>Epikarst Store</i> (via <i>F1</i>), provided the storage capacity of the <i>Epikarst</i> (Epi_{max}) is not exceeded. |
| <i>F2</i> | Drainage from <i>Store 1</i> to <i>UnderFlow Store</i> , described by a proportional drainage function whereby 40% of <i>Store 1</i> drains to the <i>UnderFlow Store</i> in any time-step. |
| <i>F3</i> | Outflow from the <i>Epikarst Store</i> which is described by a proportional drainage function ($\text{Epikarst water storage}/\text{Epi}_{\text{max}}$ multiplied by the 0.1) enabling flows of 10% of the storage volume when the reservoir is full. |
| <i>F4</i> | Water movement only occurs when the temperature is $>0^{\circ}\text{C}$. This flux enables percolating waters from the surface to bypass the <i>Epikarst</i> and flow directly to <i>Store 1</i> to prevent Epi_{max} being exceeded. These flows are likely under two situations: i. when the epikarst store is almost full; and ii. when hydrologically-effective precipitation is very high in any time-step. |
| <i>F5</i> | Overflow from <i>Store 1</i> to <i>OverFlow Store</i> : occurs when water storage in <i>Store 1</i> > 120 mm. |
| <i>F6</i> | Drainage from <i>UnderFlow Store</i> : representing water lost from the model by, for example, seepage or cave drip-waters. Flow is equal to 10% of the storage volume in any time-step. |
| <i>F7</i> | Preferential flow from the <i>Epikarst</i> to the <i>OverFlow Store</i> for time-steps when <i>F1</i> exceeds a given threshold (10). This enables rapid water movement to a particular water reservoir when hydrologically-effective precipitation is high. |
| <i>F8</i> | Drainage from <i>OverFlow Store</i> : representing water lost from the model by, for example, seepage or drips to caves. Flow is equal to 10% of the storage volume in any time-step. |
| <i>F9</i> | Evapotranspiration from <i>Epikarst</i> – occurs whenever surface evapotranspiration exceeds precipitation and described by an exponential function of the storage volume. |

These comprised monthly mean temperature and precipitation, and potential evapotranspiration (PET), estimated by the Thornthwaite equation (Thornthwaite, 1948), and the $\delta^{18}\text{O}$ composition of precipitation. For NW Scotland, climate data are available from Proctor et al. (2000) and Fuller (2007) while rainfall isotope data are from the IAEA site at Valentia. The latter were adjusted to provide a local estimate of precipitation $\delta^{18}\text{O}$ using the correlation described by Fuller et al. (2008) from an analysis of 18-months data. At Gibraltar, climate and precipitation isotope data were all derived from the local research site (Mattey et al., 2008), while for Ethiopia, climate and precipitation isotope data are all from Addis Ababa, with precipitation adjusted to reflect monthly totals in the Mechara cave region (Baker et al., 2007). At each site, the IAEA rainfall data series was incomplete, and for months where $\delta^{18}\text{O}$ is missing, data were in-filled by calculating a $\delta^{18}\text{O}$ value from the $\delta^{18}\text{O}$ – precipitation amount relationship for the whole data series. For each site, the same model configuration was used (i.e. identical variables, initial storage volumes etc.) with the exception of the initial $\delta^{18}\text{O}$ composition of each water reservoir. In each case this was adjusted in the second model run to approximate the mean $\delta^{18}\text{O}$ composition of the store over the simulation period.

Differences in the relative magnitude of individual water fluxes to and between the principal water reservoirs will have a number of implications for the isotopic compositions of individual water stores. Fig. 3 summarises the main water fluxes for the three regions: SE Ethiopia, NW Scotland and Gibraltar, giving the estimated hydrologically-effective precipitation for each site (derived from local precipitation and estimated evapotranspiration), and focussing on modelled water inputs to the three karst reservoirs: *Store 1*, the *OverFlow Store* and *UnderFlow Store*, plotted at the same scale across all sites. Total water fluxes are significantly less for Ethiopia, with intermittent surface-water inputs, and pulses of water movement to *Store 1*, principally through *F4*. Occasionally, in months of high recharge, piston flow appears to occur to the *OverFlow Store*, whilst drainage to the *UnderFlow Store* varies according to the quantity of water in *Store 1*. In contrast, in NW

Scotland, individual water fluxes are significantly greater, with high flow volumes at all levels of the model, reflecting the high and continuous surface-water inputs. At Gibraltar, water movement dynamics are comparable to Ethiopia, but with occasional very high flow surface-water inputs (i.e. HEP > 400 mm in three months). At these times, piston flow occurs, with water movement to the *OverFlow Store* via *F5* being particularly important. Theoretically, the model can be expected to simulate piston flow relatively well, given the model's focus on the sequential movement of water through the system. However, matrix flow only represents a small proportion of total water movement between individual water stores, and for some stalagmites (e.g. the classic candlestick shape) that are fed by percolating waters with a low drip rate, it might be appropriate to isolate this relatively slow flow component in a revised model.

Modelled variations in the quantities of water stored in each reservoir for the three regions over the 300 month simulation period are given in Fig. 4 (top) with the $\delta^{18}\text{O}$ composition of each reservoir over the same time-scale (bottom). There are considerable differences in water storage dynamics, both between individual water reservoirs at each site, and between sites. The simulations for Ethiopia have a strong annual (12-month) cycle with reservoirs that fill and drain seasonally but which retain water during periods of low recharge (e.g. months 140–160). From month 160 onwards, the three karst water stores (*Store 1*; *UnderFlow*; *OverFlow*) have comparable seasonal high and low storage volumes, although it initially takes ~ 30 months before the *OverFlow Store* responds fully. In contrast, in NW Scotland, the *OverFlow Store* is substantially larger than the other reservoirs (3–4 times greater than both *Store 1* and the *UnderFlow Store*) whilst the quantity of water stored in the *Epikarst Store* remains consistently at around 100 mm (reflecting low evapotranspiration). At Gibraltar, the water stores respond clearly during months with very large recharge (e.g. months 123, 196, 208) with high volumes of water passing to the *OverFlow Store* in particular.

The modelled $\delta^{18}\text{O}$ composition of each water store is also illustrated in Fig. 4, with summary statistics provided in Table 2.

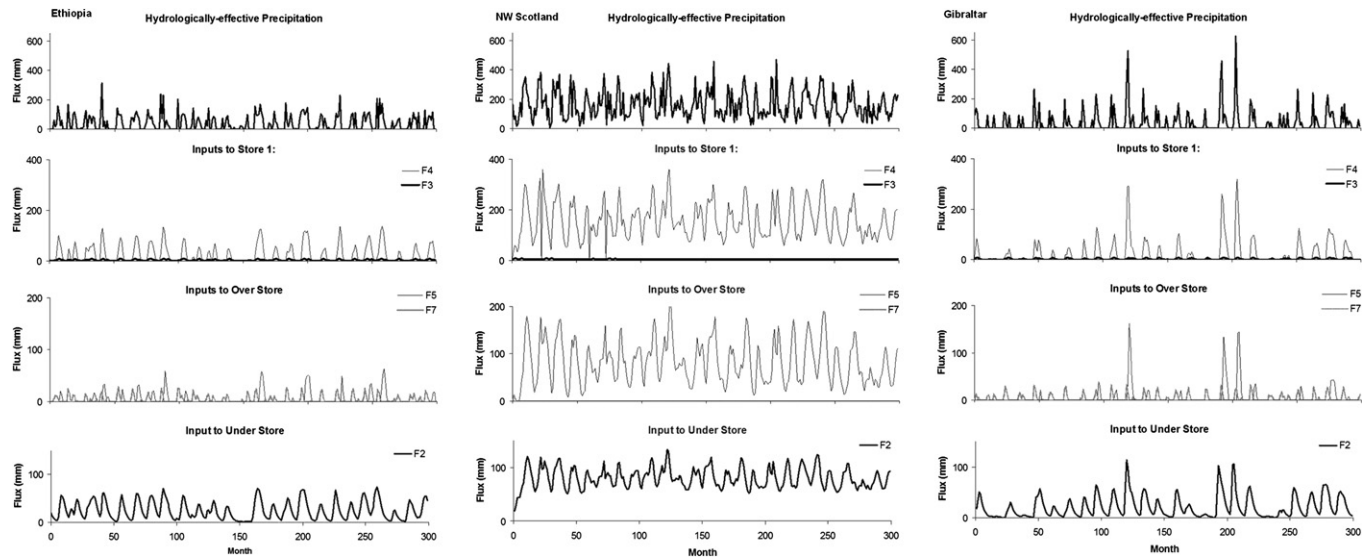


Fig. 3. Trends in water fluxes for i. Ethiopia; ii. NW Scotland; iii. Gibraltar from 1980 to 2004, comprising: estimated hydrological effective precipitation (the principal water input to the model; Top); modelled inputs to *Store 1* (F3 and F4); modelled inputs to *Overflow Store* (F5 and F7) and modelled to *UnderFlow Store* (F2).

Reservoirs that only receive occasional inflows are likely to show relatively consistent $\delta^{18}\text{O}$ values over time with a low standard deviation (e.g. *Overflow Store* in both the Ethiopian and Gibraltar model) whilst some reservoirs that fail to drain significantly have isotope compositions that approximate the long-term average, notably the *Overflow Store* in NW Scotland. The $\delta^{18}\text{O}$ composition of the *Epikarst Store* in each region is indicative of the composition of recent precipitation, and may reflect evaporative fractionation. In the model results for NW Scotland, it is noticeable that the $\delta^{18}\text{O}$ composition of *Store 1* has a strong seasonal/annual cycle, whilst the *UnderFlow Store* and *Overflow Store* have comparable isotopic compositions despite the significant differences in storage volumes between the two reservoirs. Generally, the variability in $\delta^{18}\text{O}$ composition of the water reservoirs decreases with depth, although the smallest standard deviation (Table 2) is for the *Epikarst* in NW Scotland, which remains saturated over time. Highest standard deviations are found in the *Epikarst* and *Store 1* in Ethiopia.

5. Comparison of modelled and actual stalagmite $\delta^{18}\text{O}$

Figs 5–7 compare previously published stalagmite $\delta^{18}\text{O}$ records from the three regions together with the modelled isotopic composition of each store. The comparison is undertaken for the period of overlapping model output and stalagmite isotope data, which is dependent on the length of the IAEA precipitation input series: 1962–2004 AD (Gibraltar; Fig. 5), 1969–2005 AD (Ethiopia; Fig. 6), and 1960–2005 AD (NW Scotland; Fig. 7) respectively. In all cases, the modelled drip-water composition is corrected for the temperature dependent fractionation of oxygen isotopes when incorporated into calcite using the Leng and Marshall (2004) equation which is an expression of Kim and O'Neil (1997). For the Ethiopia and Gibraltar sites, where intra-annual cave air temperature variations are minimal, we use the mean of the preceding 12 months of surface temperature. For NW Scotland, where seasonal variations in cave air temperature are observed in our study site (Fuller et al., 2008), we use the mean of

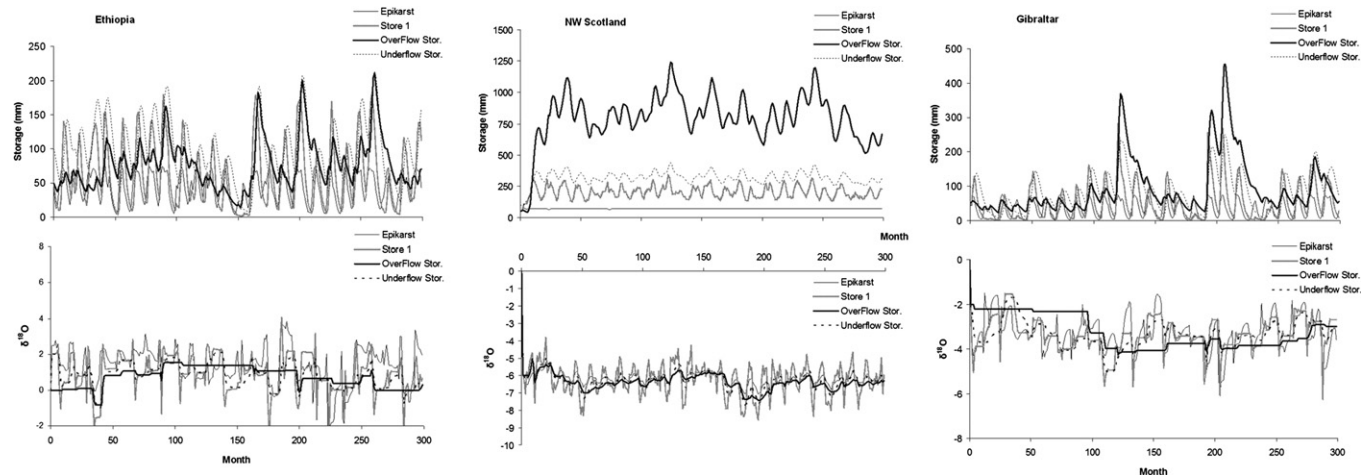


Fig. 4. Modelled variations in individual water reservoirs (*Epikarst*, *Store 1*, *Overflow*, *UnderFlow*) for the 300 months from 1980 to 2004 for i. Ethiopia; ii. NW Scotland; and iii. Gibraltar (top); and the $\delta^{18}\text{O}$ composition of each water store (bottom).

Table 2

Summary statistics indicating the variations in modelled $\delta^{18}\text{O}$ composition in the four water stores in Ethiopia (Addis), NW Scotland (Assynt) and Gibraltar to 1 decimal place (Top) with soil–water isotope fractionation (Base) without soil–water isotope fractionation.

| | Addis | | Assynt | | Gibraltar | |
|---|-------------|--------------------|-------------|--------------------|-------------|--------------------|
| | Mean (‰) | St. dev. (‰) | Mean (‰) | St. dev. (‰) | Mean (‰) | St. dev. (‰) |
| <i>With soil–water fractionation</i> | | | | | | |
| Epikarst | 1.4 | 1.1 | –6.2 | 0.3 | –3.3 | 0.8 |
| Store 1 | 0.9 | 1.1 | –6.3 | 0.9 | –3.4 | 0.8 |
| OverFlow | 0.7 | 0.6 | –6.4 | 0.4 | –3.2 | 0.7 |
| UnderFlow | 0.8 | 0.7 | –6.3 | 0.5 | –3.4 | 0.6 |
| <i>Without soil–water fractionation</i> | | | | | | |
| Epikarst | –0.3 | 1.1 | –6.7 | 0.3 | –4.2 | 0.7 |
| Store 1 | –0.7 | 1.1 | –6.8 | 0.8 | –4.4 | 0.7 |
| OverFlow | –0.7 | 0.5 | –6.9 | 0.4 | –3.9 | 1.0 |
| UnderFlow | –0.7 | 0.7 | –6.8 | 0.5 | –4.3 | 0.6 |

the preceding 3 months. No within-cave kinetic fractionation is included in our comparisons and thus the observation of stalagmite $\delta^{18}\text{O}$ that is isotopically heavier than the range modelled would allow us to infer the presence of within-cave disequilibrium deposition conditions.

At Gibraltar, we compare the stalagmite Gib-04a record with our model output. Matthey et al. (2008) sampled Gib-04a with seasonal resolution, which permits a detailed investigation of the performance of our model at this timescale. Modelled $\delta^{18}\text{O}$ series are plotted separately with Epikarst and Store 1 $\delta^{18}\text{O}$ in Fig. 5i; and OverFlow and UnderFlow $\delta^{18}\text{O}$ in Fig. 5iii. Also plotted are 6-month running means of Store 1 (Fig. 5i) and OverFlow (Fig. 5iii). The modelled series of Epikarst and Store 1 $\delta^{18}\text{O}$ successfully represents the observed variability and relative changes in stalagmite $\delta^{18}\text{O}$, which is particularly good for the running mean of Store 1 around 1990 (Fig. 5i.). Although there is relatively little variation in the OverFlow $\delta^{18}\text{O}$ series (Fig. 5iii.), these data have been used to

generate a 'compound series' of 50% OverFlow and 50% Store 1 in Fig 5iv. which gives a good agreement with the mean isotopic composition from 1988 onwards. It is noteworthy that without the inclusion of soil–water $\delta^{18}\text{O}$ fractionation, modelled $\delta^{18}\text{O}$ would be $\sim 1\text{‰}$ lighter (see Table 2) and one would then interpret the stalagmite $\delta^{18}\text{O}$ as having undergone kinetic fractionation during calcite deposition. There is no clear evidence that such fractionation has occurred. Matthey et al. (2008) notes that confirmation of this would require in-situ calcite deposition experiments, but they suggest the depositional kinetics will be climate-related. The model also captures the recent trend in stalagmite $\delta^{18}\text{O}$, with heavier isotopic composition from ~ 1995 to present, and trending to lighter values in the 1970s and 1980s. However, poorly captured is a short period of very light isotopic composition around 1970AD. This corresponds to a period when IAEA rainfall data are unavailable and long-term mean values have been used to estimate precipitation $\delta^{18}\text{O}$, and hence the disparity may simply reflect relatively light $\delta^{18}\text{O}$ of rainfall at this time, which has not been input to the model.

Matthey et al. (2008) demonstrate from monitoring data that stalagmite $\delta^{13}\text{C}$ is isotopically lightest in April of each year, and that this corresponds with the isotopically lightest stalagmite $\delta^{18}\text{O}$. They hypothesise that this is indicative of the average preceding six months $\delta^{18}\text{O}$ of precipitation. Our modelling results can be used to test this hypothesis. Fig. 5i and iii suggests that seasonal variability in stalagmite $\delta^{18}\text{O}$ falls between the modelled $\delta^{18}\text{O}$ of the UnderFlow and Store 1 components. Higher resolution modelled output in Fig. 5ii. shows that Store 1 typically has a short duration, isotopically light, water flux in each winter. This generally occurs around December or January, whilst the isotopically lightest output from the UnderFlow Store typically occurs later (in January to April), and does not occur in all years. Gib-04a does not exhibit short duration $\delta^{18}\text{O}$ excursions in winter that are as isotopically light as that modelled as coming from the Store 1, although this could in part be obscured by the stalagmite sample resolution integrating these events. Assuming that sampling

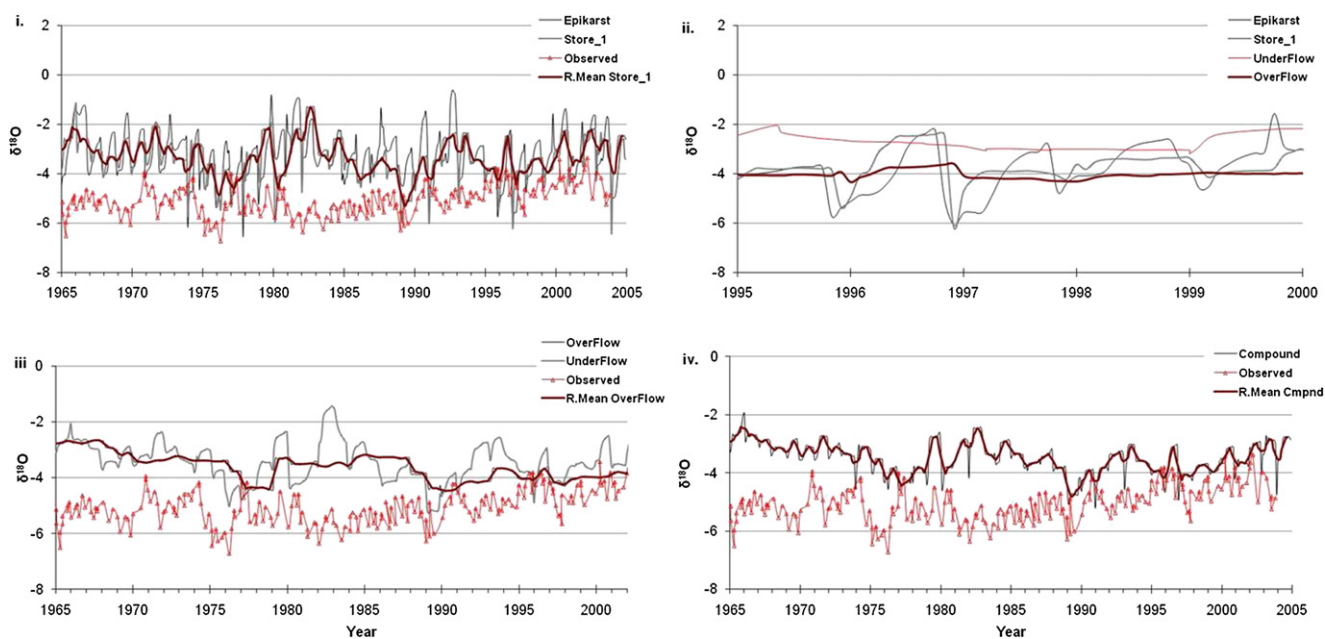


Fig. 5. Comparison of modelled isotopic composition of water store inputs with stalagmite $\delta^{18}\text{O}$ for Gibraltar. Modelled isotope composition is corrected for the temperature dependent fractionation during calcite deposition. The plots compare observed stalagmite $\delta^{18}\text{O}$ at Gibraltar with **i.** modelled Epikarst and Store 1 $\delta^{18}\text{O}$ and a 6-month running mean of Store 1; **iii.** OverFlow and UnderFlow $\delta^{18}\text{O}$ and 6-month running mean of OverFlow; **iv.** a compound $\delta^{18}\text{O}$ series comprising 50% OverFlow and 50% Store 1; and **ii.** Higher resolution model output of $\delta^{18}\text{O}$ for water stores from 1995 to 2000 AD highlighting the lagged response of the different water stores.

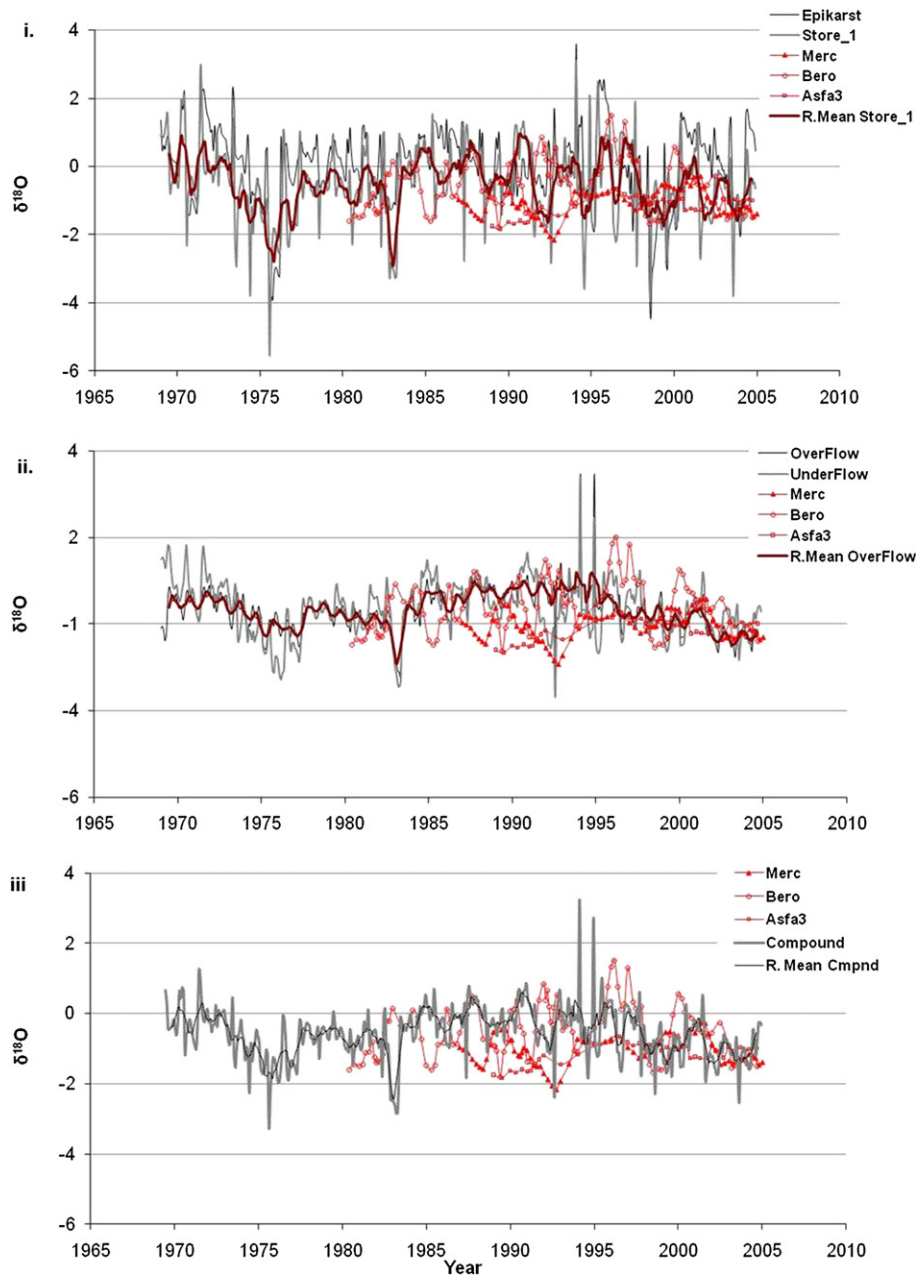


Fig. 6. Comparison of modelled isotopic composition of water store inputs with stalagmite $\delta^{18}\text{O}$ for Ethiopia (modelled isotope composition corrected for temperature dependent fractionation during calcite deposition). Plots compare point observations for three stalagmite samples (Merc-1, Asfa-3, Bero-1) with **i.** modelled *Epikarst* and *Store 1* $\delta^{18}\text{O}$, and a 6-month running mean of *Store 1*; **ii.** modelled *Overflow* and *UnderFlow* $\delta^{18}\text{O}$ and 6-month running mean of *Overflow*; and **iii.** a compound $\delta^{18}\text{O}$ series comprising 50% *Overflow* and 50% *Store 1*, with a 6-month running mean of the compound series.

resolution is not limiting stalagmite $\delta^{18}\text{O}$ variability, and that an 'April' minima in calcite $\delta^{18}\text{O}$ is indicative of a greater proportion of *UnderFlow* to *Store 1* components, then the best fit between stalagmite and model is with a mixture of these two components, with the *UnderFlow* Store providing the greater water flux. Thus our model output confirms the original premise of Matthey et al. (2008), but further suggests that inter-annual variations in the timing and amount of hydrological effective precipitation means that any simple linear regression between stalagmite $\delta^{18}\text{O}$ and preceding climate is unlikely to represent the full complexity of the actual drip-water isotopic composition reaching the stalagmite.

Fig. 6 compares model output with stalagmite data from SE Ethiopia. Stalagmites Merc-1, Asfa-3 and Bero-1 were sampled at

approximately bimonthly resolution for the last 15 yrs of deposition. The $\delta^{18}\text{O}$ record of Bero-1 has previously been modelled using a simple reservoir model which suggests that it behaves as if fed by an *Overflow* Store with waters routed from a reservoir that receives a combination of matrix and fissure flow (Baker et al., in press). Modelled $\delta^{18}\text{O}$ series from KarstHydroModel are given in Fig. 6i (*Epikarst* and *Store 1*) and 6ii (*Overflow* and *UnderFlow*), together with 6-month running means of *Store 1* and *Overflow*. The output series in Fig. 6i are characterised by considerably greater short-term variability than found in the bimonthly observations. However, the absolute range in *Overflow* $\delta^{18}\text{O}$ compares well with observed stalagmite series (Fig. 6ii), and compares more favourably than the compound series shown in Fig. 6iii. The good agreement between stalagmite and modelled *Overflow* $\delta^{18}\text{O}$, despite the lack of

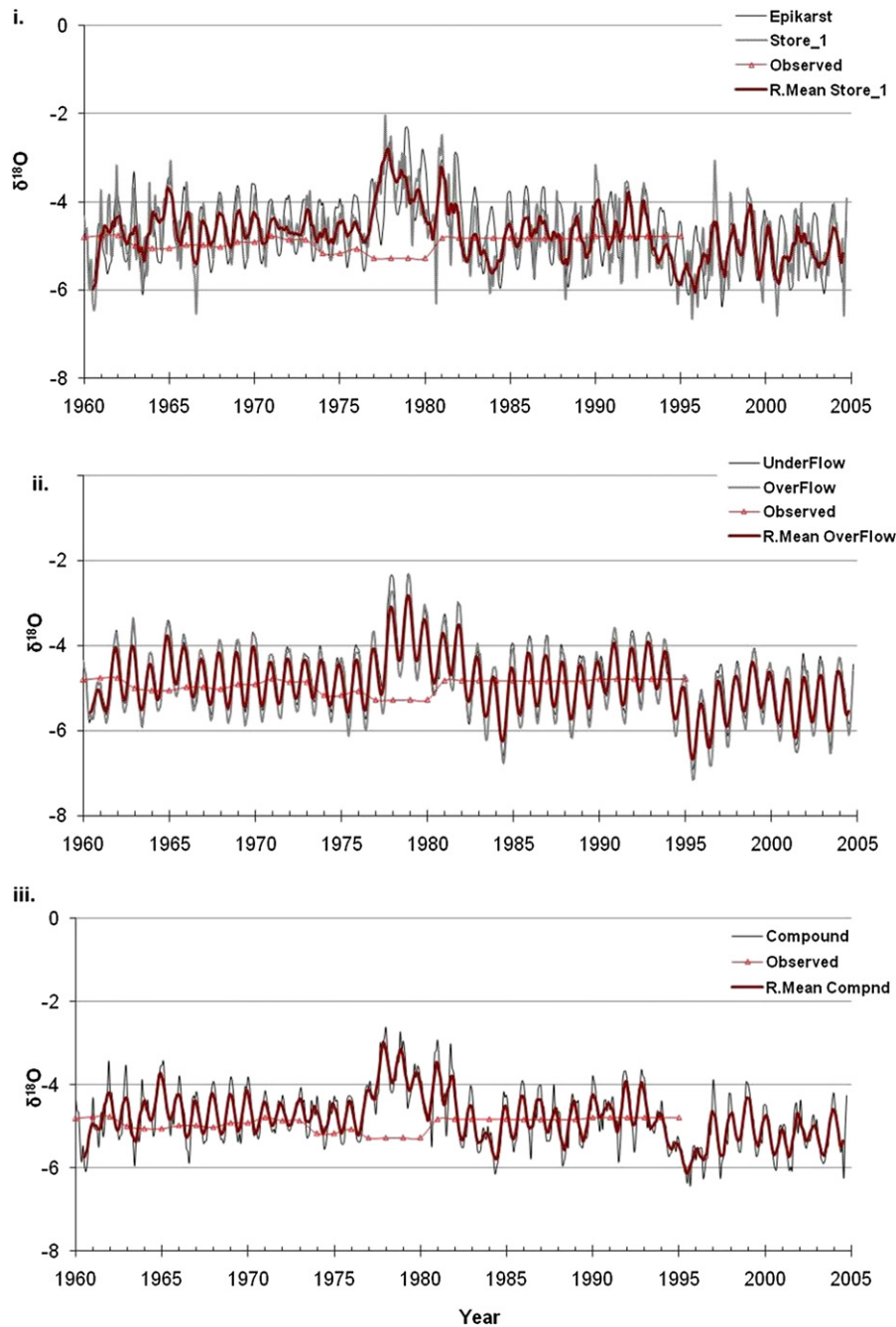


Fig. 7. Comparison of modelled isotopic composition of water store inputs with stalagmite $\delta^{18}\text{O}$ for NW Scotland (modelled isotope composition corrected for temperature dependent fractionation during calcite deposition). Plots compare point observations for one stalagmite from NW Scotland with **i.** Epikarst and Store 1 $\delta^{18}\text{O}$ and a 6-month running mean of Store 1; **ii.** UnderFlow and OverFlow $\delta^{18}\text{O}$ and 6-month running mean of OverFlow; and **iii.** a compound $\delta^{18}\text{O}$ series comprising 50% OverFlow and 50% Store 1, with a 6-month running mean of the compound series.

matrix flow component to the model, suggests that the matrix store component in Baker et al. (in press) was behaving in a similar manner to the fissure-fed reservoir represented by KarstHydroModel. Furthermore, Baker et al. (in press) did not include a soil component to the model and so did not allow for soil isotope fractionation. As a result of the latter, isotopic compositions modelled by Baker et al. (in press) were 1–2‰ lighter than observed in the stalagmite. KarstHydroModel, in contrast, accurately models the mean isotopic composition of Bero-1 using an identical soil-water isotope fractionation parameterisation to Gibraltar and NW Scotland. This suggests that ^{18}O fractionation in the soil is sufficient

to explain why the $\delta^{18}\text{O}$ composition of this stalagmite is heavier than that predicted from rainfall isotopic composition and hydrological mixing alone.

In contrast to Bero-1, Ethiopian stalagmites Merc-1 and Asfa-3, which were sampled at the same approximately bimonthly sampling resolution, are both characterised by stalagmite $\delta^{18}\text{O}$ that exhibits less sub-annual isotope variability. Stalagmite ^{18}O data from both Asfa-3 and Merc-1 fall within the range of model output $\delta^{18}\text{O}$, suggesting that both samples were deposited at, or close to, isotopic equilibrium, although water isotopic fractionation had previously taken place in the soil. Merc-1 exhibits a greater

variability than Asfa-3, which agrees with the morphology of the samples, which suggests that Merc-1 experiences fast drip rates (Baker et al., 2007). The amplitude of $\delta^{18}\text{O}$ variability for Merc-1 is of the same order of magnitude as the *UnderFlow Store* component. However, Asfa-3 $\delta^{18}\text{O}$ variability is less than that predicted by any of the KarstHydroModel stores. Baker et al. (2007) previously investigated correlations between $\delta^{18}\text{O}$ in Asfa-3 and Merc-1 and instrumental rainfall records using annually integrated $\delta^{18}\text{O}$ sampling, for the last 100 years, but failed to find any significant correlations (e.g. correlation between annual precipitation and Asfa-3 = 0.06; correlation between annual rainfall and Merc-1 = 0.13). Our sub-annual sampling, which shows less sub-annual isotopic variability than Bero-1, suggests that these two samples are fed by well-mixed waters. Comparison of the $\delta^{18}\text{O}$ times series for Merc-1 and Asfa-3 with model predicted $\delta^{18}\text{O}$ (given in Fig. 6) suggests that neither Merc-1 or Asfa-3 are hydrologically connected to the surface by any of the flow routes implemented in KarstHydroModel, which may in part explain the poor correlations with surface climate observed previously. It is very likely that a high proportion of drip-waters to one or both of these stalagmites comprises matrix flow that is not represented in our model.

Finally, Fig. 7 presents $\delta^{18}\text{O}$ data from SU-96-7 from NW Scotland. This stalagmite was sampled at a relatively coarse annual to ~ 7 year resolution, depending upon the growth rate, with the highest resolution between 1960 and 1980 AD. The presence of annual fluorescent organic matter in the stalagmite confirms the presence of direct flux from the soil, but a very slow drip rate (>1000 s per drip) and the presence of climate correlations over the decadal timescale also suggests that this stalagmite is predominantly matrix fed. KarstHydroModel does not implement a matrix flow component, and therefore one might expect a poor model to stalagmite fit in this case. However, although the most of the modelled $\delta^{18}\text{O}$ series presented in Fig. 7 are characterised by considerable short-term variability that is not evident in the stalagmite, the 6-month running mean of *Overflow* $\delta^{18}\text{O}$ in Fig. 7ii demonstrates a good agreement with mean stalagmite $\delta^{18}\text{O}$ from 1962 to 1977; and from 1986 to 1994. Notable is a period where heavier isotopic composition is predicted for the last 1970s, but where a muted response is visible in SU-96-7, 3–4 years later. In this case, the absence of a matrix storage component in KarstHydroModel is likely to be the reason for the poor temporal agreement.

6. Discussion and conclusions: implications for stalagmite palaeoclimate

Our model simulations over the timescale of a few decades exemplify how one can compare modelled drip-water $\delta^{18}\text{O}$ variability with that observed in stalagmite $\delta^{18}\text{O}$ records. Our karst hydrological modelling approach provides an estimate of the variability that can be ascribed to drip-water $\delta^{18}\text{O}$ from hydrological processes in the soil and groundwater system for the first time. This variability would be observed between stalagmites within a cave system (for example, as observed in Ethiopia for Merc-1 and Asfa-3; Fig. 6), as well as between caves within a single climate region (Merc-1, Asfa-3 and Bero-1; from two caves in Mechara, Ethiopia; Fig. 6). For the model configurations presented here, a range of drip-water $\delta^{18}\text{O}$ of up to 2‰ within a cave might be expected from hydrological considerations alone. Mean drip-water isotopic composition will also be isotopically heavier than the mean precipitation isotopic composition if soil-water evaporation is important. The latter process has been neglected in speleothem $\delta^{18}\text{O}$ studies and has important implications for our understanding of whether speleothems have undergone ‘equilibrium’ deposition,

which has previously focussed on fractionation processes within the cave (e.g. Lachniet, 2009). Our model output from Ethiopia also demonstrates how soil-water and within-cave fractionation can be differentiated.

In terms of palaeoclimate interpretation of stalagmite $\delta^{18}\text{O}$ records, our modelling demonstrates that when they are sampled (milled or drilled) at high temporal resolution (annual to multi-annual), two stalagmites might have different $\delta^{18}\text{O}$ time series, generated from the same climate input and within the range of hydrological $\delta^{18}\text{O}$ uncertainty. Hydrological modelling approaches will therefore help understand the extent to which stalagmite $\delta^{18}\text{O}$ records can be ‘wiggly matched’. Long, replicated $\delta^{18}\text{O}$ series are now starting to become available (for example, Williams et al., 2004), currently typically sampled at decadal or longer frequency. Hydrological modelling also permits the assessment of the uncertainty introduced by climate variability (such as from variations in the timing and isotopic composition of seasonal hydrologically-effective precipitation) against those generated by hydrological variations (such as from drip-waters with a relatively low storage capacity (*Store 1*) and a high proportion of fissure flow (e.g. *UnderFlow Store*)). Model output also demonstrates that the seasonal variability in precipitation $\delta^{18}\text{O}$ is likely to be expressed in drip-water $\delta^{18}\text{O}$ (presuming negligible matrix flow, which is not incorporated in KarstHydroModel). Therefore, when milled at sub-annual resolution, stalagmite $\delta^{18}\text{O}$ should preserve annual cycles, suggesting the possibility of using stalagmite $\delta^{18}\text{O}$ both as a chronological tool and as palaeoclimate proxy (as used together with stalagmite $\delta^{13}\text{C}$ by Matthey et al., 2008).

Water isotopes have recently been described as the “common currency” amongst archives of past climates, and are of increasing use in isotope enabled General Circulation Models (GCMs) (Sturm et al., 2009), as state-of-art models now permit the analysis of $\delta^{18}\text{O}$ for time periods of up to ~ 1000 years (e.g. LeGrande and Schmidt, 2009). The approach that we present here is a first step in quantifying stalagmite $\delta^{18}\text{O}$ hydrological uncertainty. As such, we hope that the hydrological modelling approaches comparable to that described here will contribute to initiatives such as the development of pseudoproxies for use in the Past Global Changes (PAGES) Paleoclimate Reconstruction Challenge (Ammann, 2008). The field of model – proxy assimilations (for example, Goosse et al., 2008) would also benefit from a better understanding of the uncertainty associated with a proxy signal such as stalagmite $\delta^{18}\text{O}$. For us, KarstHydroModel is just a first step in the development of a community stalagmite hydrological model. Future work needs to address (1) the addition of a matrix flow component to enable the modelling of very slow drip rate, ‘candlestick’ type stalagmites which are likely to be dominated by this flow routing; (2) improved parameterisation of soil isotope fractionation; (3) the inclusion of a vegetation change parameter which would permit model to represent changes in transpiration over time; (4) the coupling of model output with geochemical models of disequilibrium stalagmite deposition; and (5) the generation of long stalagmite $\delta^{18}\text{O}$ pseudoproxies linked to GCM $\delta^{18}\text{O}_p$ output. Further development of the stalagmite hydrological model will also have to consider whether time-invariant hydraulic parameters (hydraulic conductivity and porosity) can be used to model drip-water flows at longer time-scale given the degree to which karst permeability will evolve over millennial timescales. However, a future prospect is an integrated model of speleothem $\delta^{18}\text{O}$, including modelling of equilibrium and disequilibrium deposition (e.g. Romanov et al., 2008a,b; Scholz et al., 2009) and growth morphology models (for example, Kaufmann, 2003) with hydrological and soil-vegetation models.

Acknowledgements

We are grateful to two anonymous referees whose constructive comments significantly improved the final paper. AB acknowledges the support of a Durham University Institute of Advanced Study Fellowship.

Appendix. Supplementary data

Supplementary data associated with this article can be found in the online version, at doi:10.1016/j.quascirev.2010.05.017.

References

- Atkinson, T.C., 1977. Diffuse flow and conduit flow in limestone terrain in the Mendip Hills, Somerset (Great Britain). *J. Hydrol.* 35, 93–110.
- Adams, R., Parkin, G., 2002. Development of a coupled surface-groundwater-pipe network model for the sustainable management of karstic groundwater. *Environ. Geol.* 42, 513–517.
- Ammann, C., 2008. The Paleoclimate Reconstruction Challenge. *PAGES Newslett.* 16, 4.
- Bakalowicz, M., 2005. Karst groundwater: a challenge for new resources. *Hydrogeol.* 13, 148–160.
- Baker, A., Barnes, W.L., Smart, P.L., 1997. Stalagmite drip discharge and organic matter fluxes in Lower Cave, Bristol. *Hydrol. Process.* 11, 1541–1555.
- Baker, A., Barnes, W.L., 1998. Comparison of the luminescence properties of waters depositing flowstone and stalagmites at Lower Cave, Bristol. *Hydrol. Process.* 9, 1447–1459.
- Baker, A., Asrat, A., Fairchild, I.J., Leng, M.J., Thomas, L.E., Widmann, W., Jex, C., Dong, B., Calsteren, P.V., Bryant, C. Decadal scale rainfall variability in Ethiopia recorded in an annually laminated, Holocene-age, stalagmite. *The Holocene*, in press.
- Baker, A., Bradley, C., 2010. Modern stalagmite $\delta^{18}\text{O}$: instrumental calibration and forward modelling. *Global Planet. Change* 71 (3–4), 201–206.
- Baker, A., Brunson, C., 2003. Non-linearities in drip water hydrology: an example from Stump Cross Caverns, Yorkshire. *J. Hydrol.* 277, 151–163.
- Baker, A., Asrat, A., Fairchild, I.J., Leng, M.J., Wynn, P.M., Bryant, C., Genty, D., Umer, M., 2007. Analysis of the climate signal contained within $\delta^{18}\text{O}$ and growth rate parameters in two Ethiopian stalagmites. *Geochim. Cosmochim. Acta* 71, 2975–2988.
- Barrett, M.E., Charbeneau, R.J., 1997. A parsimonious model for simulating flow in a karst aquifer. *J. Hydrol.* 196, 47–65.
- Bear, J., 1972. *Dynamics of Fluids in Porous Media*. Elsevier, New York, 764 pp.
- Bowen, G.J., Wilkinson, B., 2002. Spatial distribution of $\delta^{18}\text{O}$ in meteoric precipitation. *Geology* 30, 315–318.
- Celle-jeanton, H., Travi, Y., Blavoux, B., 2001. Isotopic typology of the precipitation in the Western Mediterranean region at three different time scales. *Geophys. Res. Lett.* 28, 1215–1218.
- Cheng, H., Edwards, R.L., Broecker, W.S., Denton, G.H., Kong, X.-G., Wang, Y.-J., Zhang, R., Wang, X.-F., 2009. Ice age terminations. *Science* 326, 248–252.
- Dreybrodt, W., Franke, H.W., 1987. Wachstumsgeschwindigkeiten und Durchmesser von kerzenstalagmiten. *Die Hohle* 38, 1–6.
- Dreybrodt, W., Lamprecht, G., 1981. Computer-simulation des wachstums von stalagmiten. *Die Hohle* 31, 11–21.
- Fairchild, I.J., Smith, C.L., Baker, A., Fuller, L., Spötl, C., Matthey, D., McDermott, F., 2006a. Modification and preservation of environmental signals in speleothems. *Earth Sci. Rev.* 75, 105–153.
- Fairchild, I.J., Tuckwell, G.W., Baker, A., Tooth, A.F., 2006b. Modelling of dripwater hydrology and hydrogeochemistry in a weakly karstified aquifer (Bath, UK): implications for climate change studies. *J. Hydrol.* 321, 213–231.
- Fléury, P., Plagnes, V., Bakalowicz, 2007. Modelling of the functioning of karst aquifers with a reservoir model: application to Fontaine de Vaucluse (South of France). *J. Hydrol.* 345, 38–49.
- Ford, D., Williams, P.W., 2007. *Karst Hydrogeology and Geomorphology*. Wiley, Chichester, 562 pp.
- Franke, M.W., 1965. The theory behind stalagmite shapes. *Stud. Speleol.* 1, 89–95.
- Fuller, L., 2007. High resolution multiproxy geochemical Holocene climate records from 1000-year old Scottish stalagmites. Unpublished Ph.D. Thesis. University of Birmingham, UK, 430 pp.
- Fuller, L., Baker, A., Fairchild, I.J., Spötl, C., Marca-Bell, A., Rowe, P., Dennis, P.F., 2008. Isotope hydrology of dripwaters in a Scottish cave and implications for stalagmite palaeoclimate research. *Hydrol. Earth Sys. Sci.* 12, 1065–1074.
- Gams, I., 1981. Contribution to morphometrics of stalagmite. In: *Proceedings of the 8th International Congress of Speleology*, pp. 276–278.
- Gat, J.R., 1996. Oxygen and hydrogen isotopes in the hydrologic cycle. *Annu. Rev. Earth Planet. Sci.* 24, 225–262.
- Genty, D., Deflandre, G., 1998. Drip flow variations under a stalactite of the Pere Noel cave (Belgium). Evidence of seasonal variations and air pressure constraints. *J. Hydrol.* 211, 208–232.
- Goosse, H., Mann, M.E., Renssen, H., 2008. What we can learn from combining palaeoclimate proxy data and climate model simulations of past centuries? In: Battarbee, R., Binney, H. (Eds.), *Natural Climate Variability and Global Warming: A Holocene Perspective*. Blackwell, Oxford, pp. 163–188.
- Gunn, J., 1974. A model of the karst percolation system of waterfall swallet, Derbyshire. *Trans. BCRA* 1 (3), 159–164.
- Gunn, J., 1983. Point-recharge of limestone aquifers – a model from New Zealand karst. *J. Hydrol.* 61, 19–29.
- Hoffmann, D.L., 2008. ^{230}Th isotope measurements of femtogram quantities for U-series dating using multi ion counting (MIC) MC-ICPMS. *Int. J. Mass Spectrom.* 275, 75–79.
- Hsieh, J.C.C., Chadwick, O.A., Kelly, E.F., Savin, S.M., 1998. Oxygen isotopic composition of soil water: quantifying evaporation and transpiration. *Geoderma* 82, 269–293.
- Kaufmann, G., 2003. Stalagmite growth and palaeoclimate: the numerical perspective. *Earth Planet. Sci. Lett.* 214, 251–266.
- Kim, S.T., O'Neil, J.R., 1997. Equilibrium and nonequilibrium oxygen isotope effects in synthetic carbonates. *Geochim. Cosmochim. Acta* 61, 3461–3475.
- Lachniet, M.S., 2009. Climatic and environmental controls on speleothem oxygen-isotope values. *Quaternary Sci. Rev.* 28, 412–432.
- LeGrande, A.N., Schmidt, G.A., 2009. Sources of Holocene variability of oxygen isotopes in palaeoclimate archives. *Climate Past* 5, 441–455.
- Leng, M.J., Marshall, J.D., 2004. Palaeoclimate interpretation of stable isotope data from lake sediment archives. *Quaternary Sci. Rev.* 23, 811–831.
- Long, A.J., 2009. Hydrograph separation for karst watersheds using a two-domain rainfall-discharge model. *J. Hydrol.* 364, 249–256.
- Mattey, D., Lowry, D., Duffet, J., Fisher, R., Hodge, E., Frisia, S., 2008. A 53 year seasonally resolved oxygen and carbon isotope record from a modern Gibraltar speleothem: reconstructed drip water and relationship to local precipitation. *Earth Planet. Sci. Lett.* 269, 80–95.
- McDermott, F., 2004. Palaeoclimate reconstruction from stable isotope variations in speleothems: a review. *Quaternary Sci. Rev.* 23, 901–918.
- Moberg, A., Mohammad, R., Mauritsen, T., 2008. Analysis of the Moberg et al. (2005) hemispheric temperature reconstruction. *Climate Dynam.* 31, 957–971.
- Newton, M.D., 1973. The hydrology of limestone caves. *Cave Science. J. Brit. Speleol. Assoc.* 50, 1–12.
- Noone, D., Sturm, C., 2010. Comprehensive dynamical models of global and regional water isotope distributions. In: West, J.B., Bowen, G.J., Dawson, T.E., Tu, K.P. (Eds.), *Isoscapes: Understanding Movement, Pattern, and Process on Earth Through Isotope Mapping*. Springer (Chapter 10) 487 pp.
- Pinault, J.-L., Plagnes, V., Aquilina, L., Bakalowicz, M., 2001. Inverse modelling of the hydrological and the hydrochemical behaviour of hydrosystems: characterization of karst system functioning. *Water Resour. Res.* 37 (8), 2191–2204.
- Pitty, A., 1966. An approach to the study of karst water. *U. Hull Occ. Paper in Geography*, 5.
- Pitty, A., 1968. Calcium carbonate content of karst water in relation to flow-through time. *Nature* 217, 939–940.
- Proctor, C.J., Baker, A., Barnes, W.L., Gilmour, M., 2000. A thousand year speleothem proxy record of North Atlantic climate from Scotland. *Climate Dynam.* 16, 815–820.
- Robertson, J.A., Gazis, C.A., 2006. An oxygen isotope study of seasonal trends in soil water fluxes at two sites along a climate gradient in Washington State (USA). *J. Hydrol.* 328, 375–387.
- Romanov, D., Kaufmann, G., Dreybrodt, W., 2008a. $\delta^{13}\text{C}$ profiles along growth layers of stalagmites: comparing theoretical and experimental results. *Geochim. Cosmochim. Acta* 72, 438–448.
- Romanov, D., Kaufmann, G., Dreybrodt, W., 2008b. Modeling stalagmite growth by first principles of chemistry and physics of calcite precipitation. *Geochim. Cosmochim. Acta* 72, 423–437.
- Sanz, E., López, J.J., 2000. Infiltration measured by the drip of stalactites. *Ground Water* 38 (2), 247–253.
- Scholz, D., Mühlinghaus, C., Mangini, A., 2009. Modelling $\delta^{13}\text{C}$ and $\delta^{18}\text{O}$ in the solution layer on stalagmite surfaces. *Geochim. Cosmochim. Acta* 73, 2592–2602.
- Shurbaji, A.R.M., Phillips, F., 1995. A numerical model for the movement of H_2O , $\text{H}_2\text{O}-\text{H}_2$, and $(\text{H}_2\text{O})-\text{H}_2$ in the unsaturated zone. *J. Hydrol.* 171, 125–142.
- Segele, Z.T., Lamb, P.J., Leslie, L.M., 2009. Seasonal-to-interannual variability of Ethiopia/Horn of Africa monsoon. Part I: associations of wave-filtered large-scale atmospheric circulation and global sea surface temperature. *J. Clim.* 22, 3396–3421.
- Shuster, E.T., White, W.B., 1971. Seasonal fluctuations in the chemistry of limestone springs: a possible means for characterising carbonate aquifers. *J. Hydrol.* 14, 93–128.
- Smart, P.L., Friederich, H., 1987. Water movement and storage in the unsaturated zone of a maturely karstified carbonate aquifer, Mendip Hills, England. In: *Proceedings of the Conference on Environmental Problems in Karst Terranes and their Solutions*. National Water Well Association, Dublin, Ohio, pp. 59–87.
- Spötl, C., Matthey, D., 2006. Stable isotope microsampling of speleothems for palaeoenvironmental studies: a comparison of microdrill, micromill and laser ablation techniques. *Chem. Geol.* 235 (1–2), 48–58.
- Sturm, C., Zhang, Q., Noone, D., 2009. An introduction to stable water isotopes in climate models: benefits of forward proxy modeling for paleoclimatology. *Climate Past Discuss.* 5, 1697–1729.
- Tang, K., Feng, X., 2001. The effect of soil hydrology on oxygen and hydrogen isotopic compositions of plants' source water. *Earth Planet. Sci. Lett.* 185, 355–367.
- Taylor, S.J., Greene, E.A., 2008. Hydrogeologic characterization and methods used in the investigation of karst hydrology. In: Rosenberry, D.O., LaBaugh, J.W. (Eds.), *Field*

- Techniques for Estimating Water Fluxes Between Surface Water and Groundwater, pp. 75–114 (US Geological Survey Techniques and Methods 4-D2, Chapter 3).
- Teutsch, G., 1993. An extended double-porosity concept as a practical modelling approach for a karstified terrain. In: Hydrogeological Processes in Karst Terranes. Proceedings of the Antalya Symposium and Field Seminar, October 1990, vol. 207. IAHS Publication, pp. 281–292.
- Thi ry, D., 1988. Forecast changes in piezometric levels by a lumped parameter model. *J. Hydrol.* 97, 129–148.
- Thornthwaite, C.W., 1948. An approach toward a rational classification of climate. *Geogr. Rev.* 38 (1), 55–94.
- Tooth, A.F., Fairchild, I.J., 2003. Soil and karst aquifer hydrological controls on the geochemical evolution of speleothem-forming drip waters, Crag Cave, south-west Ireland. *J. Hydrol.* 273, 51–68.
- Trouet, V., Esper, J., Graham, N.E., Baker, A., Scourse, J.D., Frank, D.C., 2009. Persistent positive North Atlantic Oscillation mode dominated the Medieval Climate Anomaly. *Science* 324, 78–80.
- Walker, A., Crout, N., 1997. ModelMaker. Cherwell Scientific Publishing Limited, Oxford, UK.
- Wang, Y.J., Cheng, H., Edwards, R.L., King, X.G., Shao, X.H., Chen, S.T., Wu, J.Y., Jiang, X.Y., Wang, X.F., An, Z.S., 2008. Millennial and orbital scale changes in East Asian monsoon over the past 224,000 years. *Nature* 451, 1090–1093.
- White, W.B., 1969. Conceptual models for carbonate aquifers. *Ground Water* 7 (3), B97515–B97521.
- White, W.B., 2002. Karst hydrology: recent developments and open questions. *Eng. Geol.* 65, 85–105.
- Williams, P.W., King, D.N.T., Zhang, J.X., 2004. Speleothem master chronologies: combined Holocene ¹⁸O and ¹³C records from the North Island of New Zealand and their palaeoenvironmental interpretation. *The Holocene* 14, 194–208.
- Williams, P.W., 2008. The role of the epikarst in karst and cave hydrogeology: a review. *Int. J. Speleol.* 37 (1), 1–10.
- Worthington, S.R.H., Ford, D.C., 2009. Self-organized permeability in carbonate aquifers. *Ground Water* 47 (3), 326–336.
- Worthington, S.R.H., Gunn, J., 2009. Hydrogeology of carbonate aquifers: a short history. *Ground Water* 47 (3), 462–467.
- Yamada, M., Ohsawa, S., Matsuoka, H., Watanabe, Y., Brahmantyo, B., Maryunani, K. A., Tagami, T., Kitaoka, K., Takemura, K., Yoden, S., 2008. Derivation of travel time of limestone cave drip water using tritium/helium method. *Geophys. Res. Lett.* 35, 8 (Art. No. L08405).
- Zimmerman, U., Ehhalt, D., Munnich, K.O., 1967. Soil water movement and evapotranspiration: changes in the isotopic composition of the water. In: Proceedings of the Isotope Hydrology Symposium, 14–18, International Atomic Energy Authority, Vienna, pp. 567–584.